RETROFITTING AN EXISTING HELICOPTER WITH eVTOL CAPABILITIES: CHALLENGES AND OPPORTUNITIES

Lakshmi N. Sankar Aishwerya Gahlot Mark F. Costello
School of Aerospace Engineering, Georgia Institute of Technology, Atlanta, GA, USA
lsankar@ae.gatech.edu aishwerya@gatech.edu mark.costello@aerospace.gatech.edu
2.
Kyle B. Collins
Embry Riddle Aeronautical University, Daytona Beach, FL, USA
collink9@erau.edu

ABSTRACT

Over the past decade, considerable work has also been done on the design, development, and deployment of eVTOL vehicles for civilian and military use. Relatively less work has been done on retrofitting existing helicopters with eVTOL capabilities. Keeping the existing airframe while implementing changes to the structural elements, rotors, and other components such as engines and drive train presents a significant challenge. For commercial helicopters, the cost and gross weight of the system, and the impact of design changes on the performance of the vehicle must also be addressed. In this study, we examine the environmental impact of retrofitting notional helicopter configurations based on the highly successful MBB Bo 105 helicopter, and its successor, the EC 135 helicopter. The advances include an improved rotor, fuselage drag reduction technologies, and an all-electric system. Results are presented for the impact of these modifications on the system weight, range, and endurance. The paper also discusses challenges and opportunities associated with these design modifications.

1. INTRODUCTION

Over the past decade there has been considerable progress in the availability of computational tools for conceptual and preliminary design of helicopters. Advanced computational fluid dynamics and finite element analyses are also being used to retrofit existing helicopters with more efficient components. The design processes tools capable of designing conventional rotorcraft and tilt-rotor vehicles, as well as autonomous rotorcraft systems are now readily available[1-4]. Work has also been done on the design, development, and deployment of eVTOL vehicles for civilian and military use[5-10]. Johnson and Silva have conducted an excellent recent survey of these advances[11].

Relatively less work has been done on retrofitting existing helicopters with eVTOL capabilities. Keeping the existing airframe while implementing changes to the structural elements, rotors, and other components such as engines and drive train presents a significant challenge. For commercial helicopters, the cost and gross weight of the system, and the impact of design changes on the performance of the vehicle must also be addressed.

2. SCOPE OF THE PRESENT STUDY

In this study, we examine the environmental impact of retrofitting a notional helicopter based on the highly successful MBB Bo 105 helicopter and its successor, the Eurocopter EC 135 helicopter. In addition to an all-electric system, related technologies such as improved rotors, fuselage drag reduction technologies, are considered in an effort to reduce the power requirements of the system and reduce its environmental impact. Representative results that build on our earlier work[12], are presented for the impact of these modifications on the system weight, range, and endurance.

3. NOTIONAL VEHICLE PROPERTIES

The notional helicopter considered in this work is loosely based on the Bo105 helicopter (4 passengers plus a pilot), and its derivative, the EC 135 helicopter (5 passengers plus a pilot). The term "notional" is used here since most of the properties required for a detailed analysis were not available in the public domain and had to be estimated. Therefore, the performance characteristics of the notional system reported in this study may differ from the BO-105 and EC 135 helicopters in significant ways.

Appendix A presents the basic characteristics of these two notional vehicles extracted from publicly available Eurocopter technical data[13,14].

The two turboshaft engines used by the BO-105 produce a maximum power of ~ 420 HP and a continuous power of 370 HP each at sea level. The EC-135 helicopter uses twin engines with a continuous power of 562 HP each. It was assumed that 10% of the power during hover and 20% of the available power is needed to meet other operational needs and installation and transmission losses. Thus, the total continuous power available for these two aircraft is 770 HP in hover and 700 HP in forward flight for the notional helicopter I (based on Bo-105). The corresponding values are 1000 HP in hover and 940 HP in forward flight for the notional helicopter II (based on EC 135). For the present study, it was also assumed these vehicles operate in forward flight at a nominal altitude of 5,000 feet. The available power is corrected for density ratio.

The main and tail rotor solidity σ values were estimated from the drawings given in Appendix A and B. For preliminary flight performance estimates, an airfoil sectional drag coefficient of 0.008 was used for both the main and tail rotor. The equivalent flat plate area was estimated to be 14 square feet for the notional helicopter 1, and 18 square feet for the notional helicopter 2 in view of the latter's larger fuselage cross section area. These values are based on empirical curve-fits of this property as a function of vehicle weight[15].

4. PRELIMINAARY PERFORMANCE MODELS FOR THE NOTIONAL VEHICLES

The performance of the baseline vehicles was estimated from a classical text-book approach. The main power coefficient $C_{P,\text{ main rotor}}$ was first estimated as

$$C_{P,main\,rotor} = \kappa\lambda_i + \sigma\frac{C_d}{8}(1 + 4.6\mu^2) \quad (1)$$

Here κ is the induced velocity correction factor (set to 1.10) and μ is the advance ratio, defined as the forward speed V divided by the main rotor speed. The induced velocity ratio λ_i was iteratively computed from Glauert's inflow model using the following relationship:

$$C_T = 2\lambda_i\sqrt{(\mu^2 + (\mu tan\alpha_{TPP} + \lambda_i)^2)} \quad (2)$$

Here α_{TPP} is the forward tilt of the tip path plane for the rotor to provide propulsive force in the flight direction. This angle may be estimated from the vehicle drag (based on flight velocity and equivalent flat plate area f) and the vehicle weight.

The power and thrust coefficients, C_P, and C_T, are defined in terms of the rotor power P, and thrust T (approximately equal to the gross weight of the vehicle) in terms of density (at a specified altitude), advance ratio μ (defined as the forward speed by rotor tip speed), rotor disk area A, rotor angular velocity Ω, and the rotor radius R as follows:

$$C_T = \frac{T}{\rho A(\Omega R)^2} \qquad C_P = \frac{P}{\rho A(\Omega R)^3} \quad (3)$$

Once the main rotor power was known, it was divided by the main rotor angular velocity Ω to obtain the main rotor torque Q. From the main rotor torque and the distance between the main and tail rotor shafts, the tail rotor thrust was estimated. The tail rotor power was subsequently

computed using the same formulas as for the main rotor.

The fuselage parasite power was estimated, in terms of the estimated equivalent flat plate area f (non-dimensionalized by the main rotor disk area A) and the advance ratio μ as follows:

$$C_{P,parasite} = \frac{1}{2}\frac{f}{A}\mu^3 \quad (4)$$

The total power was estimated as the sum of the main and tail rotor power, plus the parasite power. In hover calculations, the advance ratio is set to zero.

The rate of climb is estimated from the excess power (difference between the available power corrected for density ratio and auxiliary power requirements, and the required power) divided by the vehicle weight. The service ceiling was estimated as the altitude at which the rate of climb is approximately 100 feet per minute. Maximum forward speed at a specified altitude is estimated as the forward velocity V at which there is no excess power. In this study, these calculations were done at an altitude of 5000 feet.

The vehicle range and endurance were also estimated by numerical integration as follows. In the equation below, *sfc* is the specific fuel consumption of the engine in pounds of fuel burned per hour per unit horsepower, vehicle weight W is given in pounds, and the forward velocity V of the vehicle is specified in mph or in knots. Cruise speed is determined as the forward speed that maximizes range. Endurance speed is determined as the speed V at which the power required is minimized.

$$Range = \int_{Start}^{end} V\frac{DW}{(sfc)P} \quad (5)$$

$$Endurance = \int_{Start}^{end} \frac{DW}{(sfc)P}$$

A spreadsheet-based model of the vehicle power requirements and performance has been developed using the approach above. For range and endurance calculations, the integrands were evaluated at the mid-point of the flight, where half the fuel has been consumed.

5. COMPARISONS OF PREDICTED PERFORMANCE WITH PUBLISHED DATA

For the notional configuration 1, a gross weight of 5,500 lbs, composed of 3,500 lbs in empty structural weight, 990 lbs of fuel, and 1,010 lbs of payload was used. With a maximum power of 840 HP at sea level, the service hover ceiling out of ground effect is 6100 feet at standard atmospheric conditions. This value is within 2% higher than the published value of 6000 feet shown in Figure 5-10 in Ref. 13.

Figure 1 shows the variation of range with vehicle forward velocity. The computed range at 5000 feet, with a gross weight of 5500 lb and a fuel weight of 990 lbs is 361 nautical miles, roughly 6% higher than the published value of 340 nautical miles given in Figure 9.3 of Ref. 13. If 10% of the fuel is treated as reserve, then the estimated range is comparable to the published data.

The computed endurance of 4 hours and 20 minutes is considerably higher than the reported value of 3 hours and 45 minutes[13].

The service ceiling for the notional helicopter model 2 under a maximum power of 1000 HP is 7700 feet, roughly 500 feet above the published data, page 45 of EC 135 Technical data[14].

Calculations for the notional helicopter model 2 (using a fuel weight of 1179 lb and an average mid-way point weight of 5660 lb) at an altitude of 5000 feet. Figure 2 shows the predicted range as a function of forward velocity, yield a range of 364 nautical miles at an altitude of 5000 feet at a cruise speed of 110 knots. If 10% of the fuel is reserved for emergency use, the predicted range is 330 nautical miles. This value closely matches the 332 nautical mile range reported in the EC 135 Technical Data document[14]. The computed

endurance of 4 hours 20 minutes at 5000 feet altitude is considerably higher than the published value of 3 hours and 30 minutes in the EC 135 technical data document.

In summary, the textbook performance model described above gives reasonable results for hover ceiling and range for both the notional helicopter configurations at an operating altitude of 5000 feet. However, the predicted endurance does not match well with published data for EC 135.

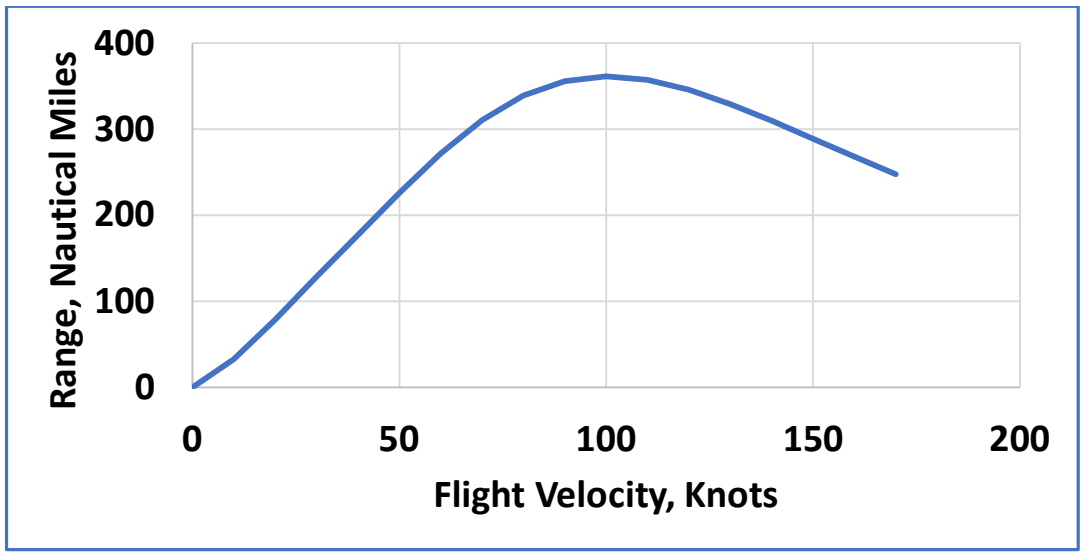

Figure 1. Variation of Range with Flight Speed for Notional Vehicle 1 at an Altitude of 5000 feet

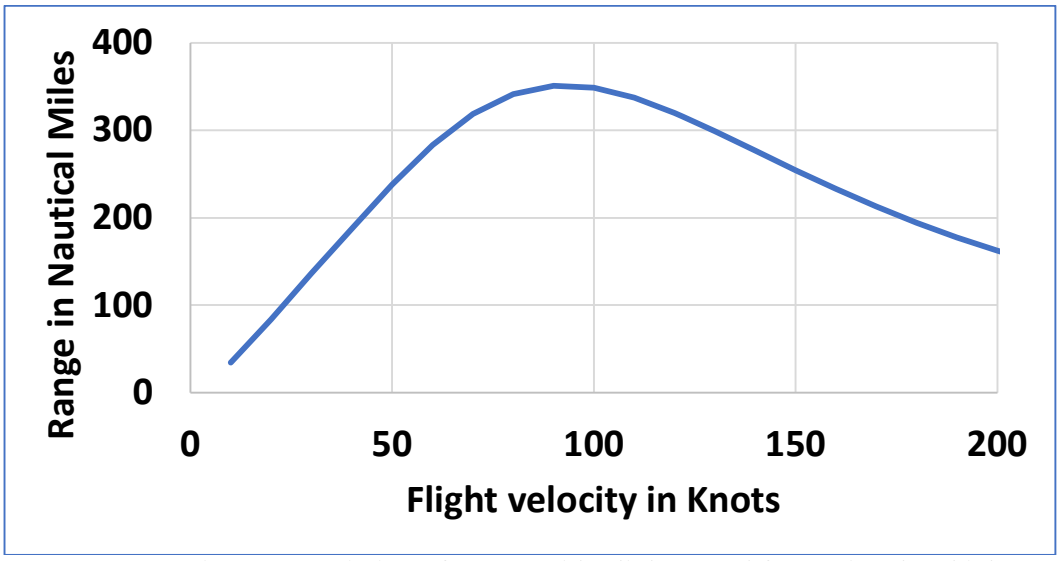

Figure 2. Variation of Range with Flight Speed for Notional Vehicle 2

6. IMPROVEMENTS TO ROTOR PERFORMANCE

The rotor blade used in EC 135 is a later generation rotor that has been optimized from

hover, cruise flight, noise, and vibration perspectives. On the other hand, the earlier generation rotor used in the first notional helicopter configuration (patterned after Bo 105) uses a rotor blade of rectangular planform, with a linear twist of -8 degrees. In an earlier work, the present researchers have attempted to redesign this rotor for improved performance[16]. This previously published approach is briefly described here.

A multi-objective/multi-fidelity approach is used as shown in Figure 3. A bi-linear variation in the geometric twist has been assumed. To preserve common features with the BO-105 configuration, much of the rotor has a constant chord length. However, a tapered (swept) tip shape with anhedral was considered as shown in Figure 4 below. The tip taper ratio, the radial location at which taper/sweep begins, and the anhedral angle are three of the design variables that may be parametrically varied. In this work, the NACA 23012 sections have been used to preserve common features with the BO-105, although other low drag airfoils may be used within the present framework.

The BO-105 rotor blades are slender and may experience significant bending and torsional deformation in hover and forward flight. In the present redesign, the mass per unit length of the blade is modified based on the square of the ratio of the local chord length to the baseline chord length. The moment of inertia is scaled by the cube of this ratio.

The primary objective of the rotor redesign design exercise is to minimize a weighted sum of the power consumption in hover and cruise, and the associated noise level at user specified locations. These quantities were normalized by the baseline values to arrive at a non-dimensional objective function. The hub vibratory loads were also monitored to ensure that the rotor redesign does not lead to excessive cabin vibrations.

Given the large number of design variables, it is necessary to screen the design space using an inexpensive low fidelity approach and identify promising candidates. In the present work, the comprehensive analysis RCAS, developed at ART, Inc.[17] was used for trimming the rotor and to estimate elastic deformations. The rotor blades are modelled using a lifting line theory within RCAS (although RCAS supports more sophisticated aerodynamic models), with a table look-up of airfoil load characteristics as a function of Mach number and sectional angle of attack. Corrections for tip losses, unsteady aerodynamics, and dynamic stall effects were incorporated. Inflow through the rotors was using a prescribed wake, augmented by dynamic inflow models. Prior to its use for redesigning the BO-105 rotor, this solver was validated against test data[16].

Noise characteristics (dB levels at user specified observed locations) were computed using PSU-WOPWOP[18]. The blade geometry is used to compute the thickness noise, while the compact airloads at the lifting line were used to predict the loading noise.

A small subset of points in the design space, which now contains several million combinations of the design variables, were examined using the high fidelity CFD tools TURNS in hover[19] and the in-house solver GT-Hybrid for forward flight[20]. The aerodynamic loads influence the blade deformations and vice versa. Therefore, a loosely coupled CFD-RCAS simulation was done. The blade deformations were supplied to the flow solver as user specified tables of vertical deformations and angular rotations at several radial locations and azimuthal locations. Several iterations between the flow solver and RCAS are needed to achieve a fully coupled CFD-RCAS solution. The airloads and blade geometry from the fully coupled simulation were used in PSU-WOPWOP to obtain the noise levels at specified locations.

These combined low- and high-fidelity simulations identified four promising configurations (that minimize a single design metric) and an optimum configuration that

minimizes the weighted objective, as shown in Figure 5.

High fidelity analyses done at the end of the design cycle indicate that the optimized rotor would reduce the rotor power required by approximately 5% in hover, and by 4% in forward flight as shown in Figure 5. Vibratory loads at the hub were also reduced.

Noise levels, as predicted by PSU-WOPWOP using high fidelity airloads indicate smaller reduction (less than 1 dB) in hover and forward flight both at most of the observer locations. Further details of the design process and the validations studies done to select the design tools are documented in Ref 16.

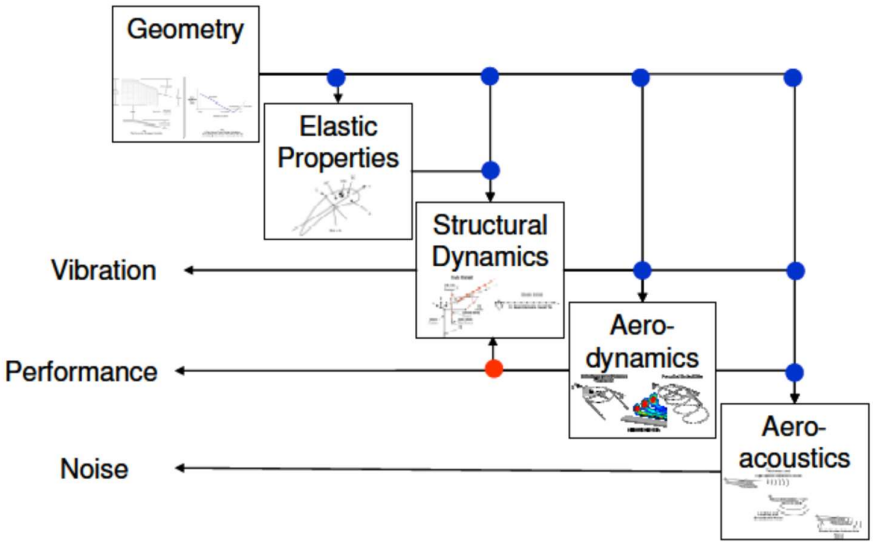

Figure 3. Multi-Disciplinary Approach for Rotor Blade Analysis and Design

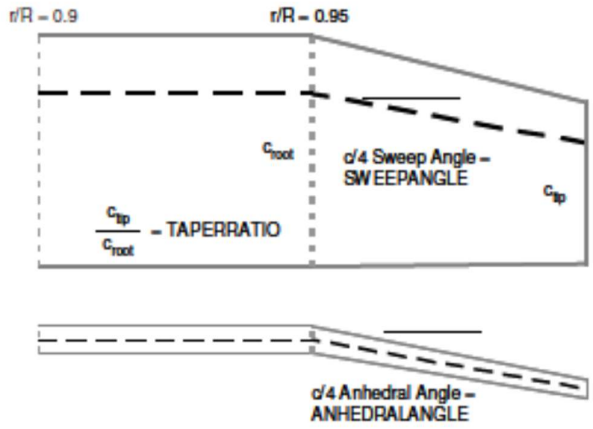

Figure 4. Rotor Planform Variables

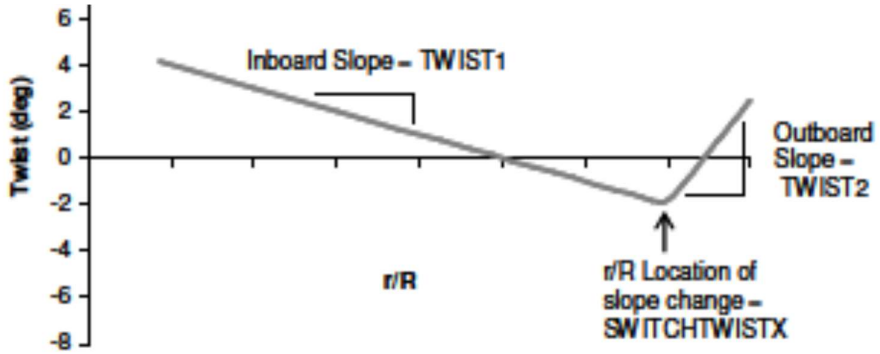

Figure 4. Rotor Blade Tip Design Variables

Design Variables	E	F	G	H	optimum
c/4 Sweep Angle	0.31	0.15	14.44	0.96	0.19
Anhedral Angle	14.59	13.84	0.63	1.19	14.56
Taper Ratio	0.71	0.60	0.62	0.61	0.60
Twist1	-17.77	-17.90	-17.65	-8.05	-12.44
SwitchTwistx	0.95	0.93	0.95	0.93	0.95
Twist2	17.42	1.55	27.17	-5.36	14.99
	min hover power	*min hover noise*	*min fwdflt power*	*min fwdflt noise*	*good compromise*

Figure 5. Minimum Noise and Lower Power Rotor Geometries Characteristics in Hover and Forward Flight for Configuration 1

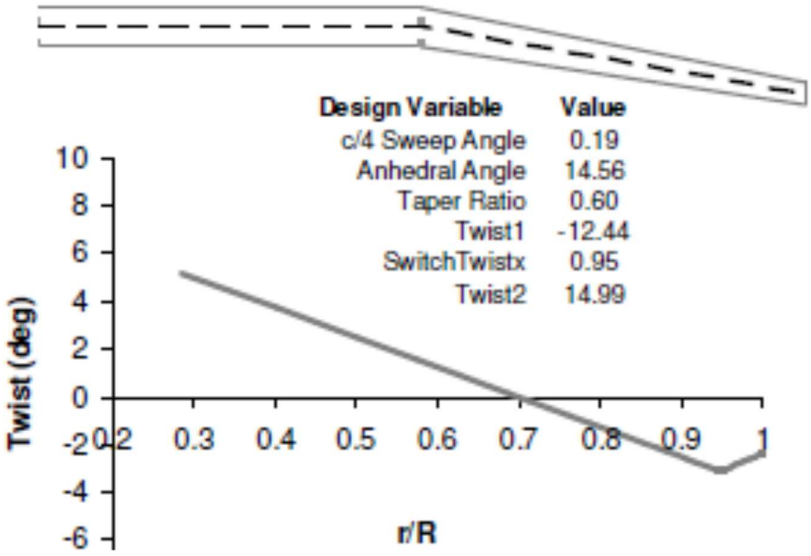

Figure 5. Optimum Anhedral and Twist (The outer 5% of the rotor has a taper ratio of 0.6)

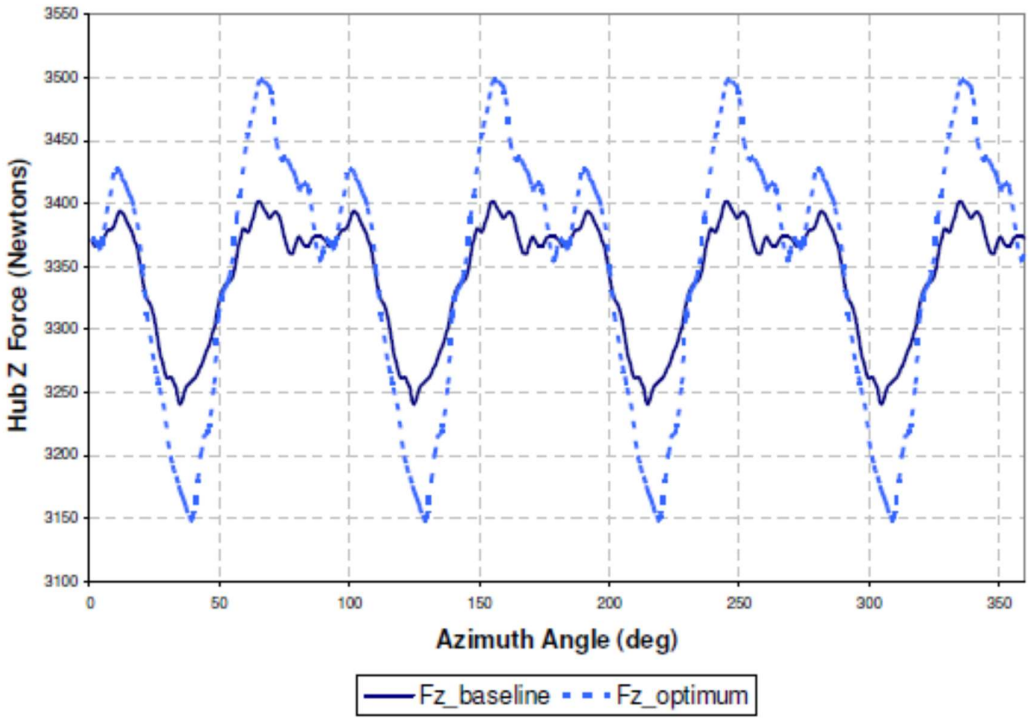

Figure 6. Reductions in the Vibratory Component of the Hub Vertical Force

7. REDUCTIONS IN VEHICLE DRAG

The B0 105 and the EC 135 helicopters both have fixed landing gears (skids) and a blunt base at the back of the fuselage. Using retractable landing gears would increase the cost, weight, and complexity of the system. The baggage compartment is located in the aft region of the fuselage, and any structural modifications to the fuselage would impede easy access to the baggage. Therefore, streamlining the fuselage is not an option.

Passive techniques for drag reduction such as the use of vortex generators in the aft region of the fuselage have some potential. However, sharp edges associated with these devices would be a concern from a passenger and baggage handlers' point of view. However, active flow control techniques, which require minimal changes to the baseline fuselage configuration, are a viable path for reducing the fuselage equivalent flat plate area. An extensive body of literature exists in this field. The most relevant to the present application is the work done at NASA[21]. The present researchers[22] have explored synthetic Coanda Jets, placed in the aft region of the fuselage, as a way of reducing the equivalent A fuselage shape similar those in use in BO-105 and several other commercial helicopters, has been considered. In this section, representative results from a previously published study[22] are presented for the Robin fuselage shown in Figure 7 are used to illustrate the potential of this technology.

Figure 7 also shows the synthetic jet slots in the aft region of the fuselage. A number of studies have been done varying the frequency and the peak blowing coefficient. In-house Navier-Stokes solvers were used, at times in combination with a Lattice Boltzmann model of synthetic jet cavities. Synthetic jets with a maximum amplitude of 20% the freestream velocity, at a frequency of 0.33 times V_∞/W, where V_∞ is the flight velocity and W is the

fuselage maximum width, were used. The momentum coefficient of the jet and the angle at which the jet leaves the injection slots were specified. To take advantage of the Coanda effect, the jets were injected at a 15-degree angle to the fuselage surface. Figure 8 shows that the fuselage drag coefficient (with the fuselage maximum cross-sectional area as the reference area) may be reduced by as much as 30% with this technology.

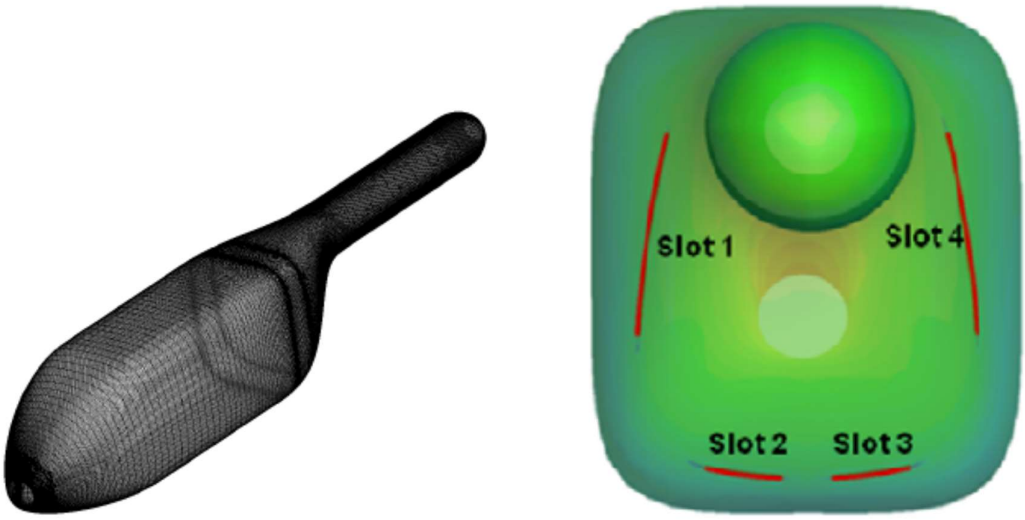

Figure 7. NASA Fuselage Configuration and Jet Slot Locations [21, 22]

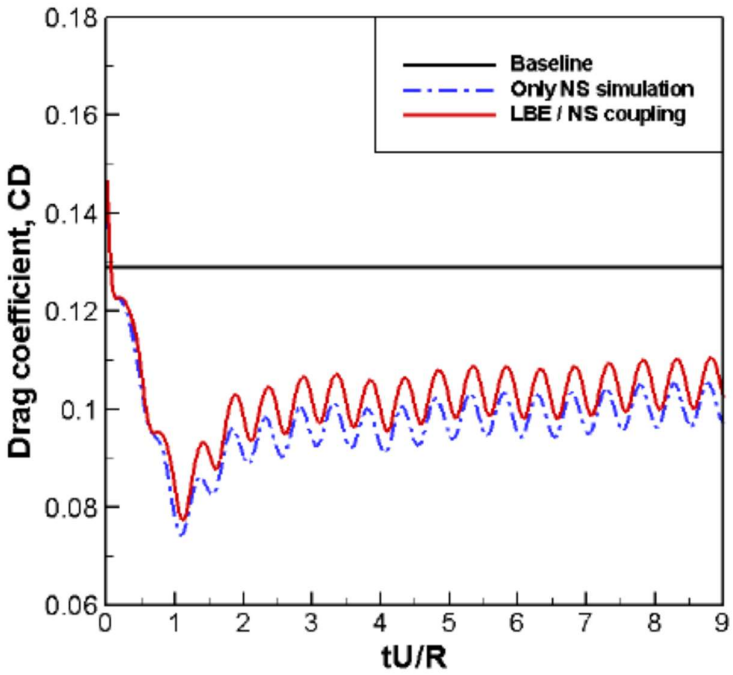

Figure 8. Effect of Synthetic Jets on Fuselage Drag Coefficient for a Representative Condition [22]

Operating the synthetic jets would require power. This power requirement may be estimated as the mass flow rate of the synthetic jet times the kinetic energy of the jet. This power consumed by the jets may be included in the performance calculations. Alternatively, a "penalty" factor

may be applied to the reduction in equivalent flat plate area. The present performance calculations using Equation (4) for the fuselage parasite power indicate that every square foot of equivalent flat plate area reduction would translate into 20 to 25 HP reduction in power consumption for the notional vehicle configurations.

8. EXPLORATION OF eVTOL TECHNOLOGIES

In the previous sections, performance models for the two notional vehicles were developed, and the computed performance (in terms of power consumption) was compared against existing rotorcraft. Modifications to the baseline rotor (for configuration 1) for reducing the rotor power consumption and active flow controls for reducing fuselage parasite power consumption were explored. In this section, techniques for further reductions in the environmental impact through the use of electric propulsion technology is explored.

Since the present study is aimed at retrofitting existing helicopters with eVTOL capability, a decision was made that many of the existing components, including the transmission system and shafts that supply power to the main and tail rotor would be retained. The two turboshaft engines, each providing 300 to 350 HP are being replaced by two electric motors supplying 250 KW (~330 HP) each. The motors are cross coupled, and the available power from a single motor is sufficient for the notional vehicles safely land in case one of the motors is inoperative (OEI). The RPM of the motors is selected to be 3600. The weight of the motors was estimated using the regression fits provided by Johnson and Silva[6]. This weight was multiplied by a technology factor of 1.65 to allow for uncertainties in the weights, and budget for the extra weight of controllers/inverters and thermal management systems. Each of these motors would weigh approximately 135 lbs after the application of the technology factor. This value is comparable to the dry weight of Allison Model 250 engine used in Bo 105 helicopter[23]. Therefore, the motor weight and the engine weight roughly offset each other.

Johnson and Silva identify some of the battery technology factors of importance for use in eVTOL systems[11]. These include cost, energy density (in watt-hours per kg of battery weight), battery volume, the ability to supply discharge current for a specified duration, and the ability to operate and deliver required power at high temperatures. As a first step, the required stored energy in the battery systems was estimated. Two missions were considered.

- Pilot plus 4 to 8 passengers (for configurations 1 and 2, respectively), 300 nautical mile range; baseline single main rotor and tail roto helicopter
- An air-taxi mission with a shorter 60 nautical mile range

A third viable option is a hybrid turbo-electric or diesel-electric system, where the electric motors would drive the main rotor and tail rotor, while the turbine engine (or a diesel engine) would provide the required electric power for driving the electric motors. The excess power from the engine would be used to charge a lower weight battery pack of smaller energy. Although fossil fuel is required with this option, the carbon footprint would likely be smaller. Such an option would be particularly attractive for distributed propulsion/lift systems. A number of established helicopter companies and eVTOL start-up companies, working in collaboration with engine companies, are considering this option[24]. In this work, this option has not been explored because of the limited information publicly available on the cost and weight of such systems.

Figure 9 below shows the various segments of the mission profile. The energy required for each segment of the profile may be estimated as the power requirement for that segment times the time elapsed in completing that segment of the mission.

Figure 10 shows the energy storage requirements, the required weight of the battery storage system (assuming 500 watt-hour per kg of energy density), The weight savings in fuel weight (1000 lbs to 1100 lb) plus the tank is assumed to be 1300 lbs for configurations 1 and 2, both. The power estimates used these tables are conservative estimates and do not include the reduction in power that may be achieved with improved rotor efficiency, and reduction in fuselage cross section area. Figure 13 indicates that an air taxi operation of 55 nautical miles (~100 km) should be feasible with these vehicles, although a longer-range vehicle is not feasible with current generation battery technology.

9. SUMMAY AND CONCLUSIONS

A study of technologies for improving the performance of two notional helicopter configurations, based on existing successful commercial helicopters has been done. The analyses are based on previous studies by the present authors and are intended to assess the impact these technologies on the environmental footprint of these vehicles.

The first technology involves replacing the existing rectangular planform rotor for the first notional configuration with a rotor that has a taper in the tip region, a bi-linear twist distribution along the length of the rotor, and anhedral. These changes would meaningfully improve the vehicle range and endurance, or alternatively reduce the fuel consumption needed to perform a typical cruise mission. The noise and vibration levels would also be reduced by a careful design of the rotor.

Use of active flow control in the rear of the fuselage, without significant impact on the baggage/storage volume or passenger/handler access was also examined. It was observed that a reduction in the fuselage parasite drag, and an improvement in the range (and/or fuel savings would be possible.

Replacement of the conventional turbine system with an all-electric system has also been examined. It was found that the energy storage in current generation batteries would not support 300+ nautical miles without a significant impact on the system gross weight. However, current generation battery technologies supplying 500 watt-hours per kilogram of battery weight appear to be well suited for shorter fifty-five nautical mile intra-city trips with both configurations.

The present study is aimed at retrofitting existing vehicles and makes many of the existing components, including the transmission system and shafts that supply power to the main and tail rotor. Removal of the tail rotor transmission shaft and use of two small motors that separately tail rotor may provide some weight savings.

A cost model of the retrofitted vehicles has not been attempted to assess the economic viability of the use of these vehicles for air taxi operations.

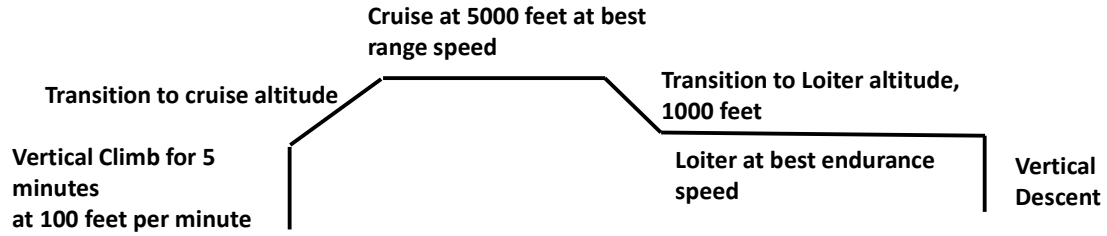

Figure 9. Typical Mission Profile

Mission Segment	300 nautical Mile, baseline mission	Air Taxi (55 nautical miles - 100 km)	Units
Take-Off Phase, 680 kW including verical climb at 100 feet per min, for 5 minutes	57	57	kW-hr
Climb to cruise altitude, cruise, descent,includes 10 KW for auxiulary system (330 kW)	990	165	kW-hr
Loiter + Emergency operations Phase at endurance speed, 270 kW, 10 minutes	45	35	kW-hr
Vertical Descent, 600 kW, 2 minutes	20	20	kw_Hr
Total Energy	1112	277	kW-hr
Battery weight, 500 watt-hr per kg	2224	554	kg
Battery weight	4892.8	1218.8	lbf
Motor weight	270	270	lbf
Engine weight savings	270	270	lbf
Fuel + tank savings	1200	1200	lbf
Net increase in gross weight	3692.8	18.8	lbf

Figure 10 a. Energy Needs and Weights Estimate (Configuration 1, 4 passengers plus a pilot)

Mission Segment	300 nautical Mile, baseline mission	Air Taxi (55 nautical miles - 100 km)	Units
Take-Off Phase, 680 kW including verical climb at 100 feet per min, for 5 minutes	57	57	kW-hr
Climb to cruise altitude, cruise, descent,includes 10 KW for auxiulary system (330 kW)	990	165	kW-hr
Loiter + Emergency operations Phase at endurance speed, 270 kW, 10 minutes	45	35	kW-hr
Vertical Descent, 600 kW, 2 minutes	20	20	kw_Hr
Total Energy	1112	277	kW-hr
Battery weight, 500 watt-hr per kg	2224	554	kg
Battery weight	4892.8	1218.8	lbf
Motor weight	270	270	lbf
Engine weight savings	270	270	lbf
Fuel + tank savings	1200	1200	lbf
Net increase in gross weight	3692.8	18.8	lbf

Figure 10 b. Energy Needs and Weights Estimate (Configuration 2, 5 passengers plus a pilot)

REFERENCES

[1] Johnson, W. NDARC — NASA Design and Analysis of Rotorcraft. Validation and Demonstration. American Helicopter Society Specialists' Conference on Aeromechanics, San Francisco, CA, January 2010.

[2] Johnson, W. NASA Design and Analysis of Rotorcraft. NASA TP 2015-218751, 2015.

[3] Silva, C., Johnson, W. and Solis, E. Multidisciplinary Conceptual Design for Reduced Emission Rotorcraft. American Helicopter Society Technical Conference on Aeromechanics Design for Transformative Vertical Flight, San Francisco, CA, 2018.

[4] Johnson, W. A Quiet Helicopter for Air Taxi Operations. Vertical Flight Society Aeromechanics for Advanced Vertical Flight Technical Meeting, San Jose, CA, January 2020.

[5] André, N. and Hajek, M. Robust Environmental Life Cycle Assessment of Electric VTOL Concepts for Urban Air Mobility, AIAA Paper No. 2019-3473, June 2019.

[6] Johnson, W. A., Silva, C., and Solis, E., Concept Vehicles for VTOL Air Taxi Operations. AHS Technical Conference on Aeromechanics Design for Transformative Vertical Flight, San Francisco, CA, 2018.

[7] Hendricks, E.S., Falck, R.D., Gray, J.S., Aretskin-Hariton, E.D., Ingraham, D.J., Chapman, J.W., Schnulo, S.L., Chin, J.C., Jasa, J.P. and Bergeson, J.D. Multidisciplinary Optimization of a Turboelectric Tiltwing Urban Air Mobility Aircraft. AIAA Paper No. 2019-3551, June 2019.

[8] Hendricks, E.S., Aretskin-Hariton, E.D., Ingraham, D.J., Gray, J.S., Schnulo, S.L., Chin, J.C., Falck, R.D. and Hall, D. L, Multi-disciplinary Optimization of an Electric Quadrotor Urban Air Mobility Aircraft. AIAA Paper No. 2020-3176, June 2020.

[9] Chakraborty, I., Mishra, A. A., and Miller, N. S., "Sizing and Analysis of a Tilt-Wing Aircraft with All-Electric and Hybrid-Electric Propulsion Systems," AIAA Sci-Tech Forum, San Diego, CA, January 3-7, 2022.

[10] Chakraborty, I., Mishra, A. A., and Miller, N. S., "Design and Sizing of a Dual-Purpose Hybrid-Electric Ducted Fan Lift-Plus-Cruise Aircraft," AIAA Sci-Tech Forum, San Diego, CA, January 3-7, 2022.

[11] Johnson, W. and Silva, C. NASA Concept Vehicles and the Engineering of Advanced Air Mobility Aircraft, The Aeronautical Journal (2022),126, pp. 59–91.

[12] Sankar, L. N., Costello, M., and Collins, K., Low and High-Fidelity Approaches for Low Noise eVTOL Modeling and Design, 56th 3AF International Conference on Applied Aerodynamics, 28 – 30 March 2022.

[13] BO 105 CB-5/CBS-5 Approved Rotorcraft Flight Manual, Eurocopter Deutschland GmbH, April 1995,

[14] Eurocopter EC 135 Technical Data, https://www.hdf.fr/public/PDF/EC_135_PDF.pdf .

[15] Leishman, J. G., Principles of Helicopter Aerodynamics, Second Edition, Cambridge Aerospace Series. 23.

[16] K. Collins, L. Sankar, D. Mavris, "Application of Low- and High-Fidelity Simulation Tools to Helicopter Rotor Blade Optimization," J. American Helicopter Society, Volume 58, Number 4, October 2013,

[17] RCAS User's Manual, Version 2.0, Technical Report USAAMCOM/AFDD TR 02-A-006, June 2003.

[18] Brentner, K. S., Bres, G. A., Perez, G., and Jones, H. E., "Maneuvering Rotorcraft Noise Prediction: A New Code for a New Problem," AHS Specialists Meeting, 2002.

[19] Srinivasan, G. and Baeder, J., TURNS: A Free-Wake Euler/Navier-Stokes Numerical

Method for Helicopter Rotors, AIAA Journal, Vol. 11, No. 5, 1992.
[20] Marpu, R., Sankar, L. N., Egolf, A., Hariharan, N., "Analysis of a Rotor in Hover using Hybrid Methodology," AIAA Paper 2014-0210.
[21] Schaeffler, N. W., Allan, B/, Lienard, C. and Le Pape, A., Progress towards Fuselage Drag Reduction via Active Flow Control: A Combined CFD and Experimental Effort, 36th European Rotorcraft Forum, 2010.
[22] Kim, J. W., Sankar, L., Zheng, C., Yeshala, N., Egolf, T., Multiscale Modeling of Active Flow Control for Fuselage Drag Reduction," AIAA 2012-0075.
[23] Allison Model 250 Specifications, https://en.wikipedia.org/wiki/Allison_Model_250
[24] Carlucci, F., "Hybrid Propulsion: Halfway to Paradise?" Vertiflite, Sept/Oct 2020.

APPENDIX A: TECHNICAL SPECS FOR THE TWO NOTIONAL HELICOPTERS

Configuration 1 (4 passengers plus pilot, 300 nautical mile range, based on Bo 105)		
HELICOPTER DATA	**Units**	
Gross Weight	lb	5500
Nb of Engines	-	2
Engine Type	-	Allison 250 C-20B
Main Rotor Diameter	ft	32.25
Number of blades	-	4
Main Rotor Chord	ft	0.945
Rotor Revolutions per Minute	RPM	424
Rotor Solidity (estimated)	-	0.07
Tail Rotor Diameter	ft	3.25
Number of blades	-	2
Tail Rotor RPM	RPM	1975
Tail Rotor Solidity (estimated)	-	0.32
Distance between rotors (Estimated)	ft	20.00

Configuration 2 (5 passengers plus pilot, 300 nautical mile range, based on EC 135)		
HELICOPTER DATA	**Units**	
Gross Weight	lb	6250
Nb of Engines	-	2
Engine Type	-	PW206B2
Main Rotor Diameter	ft	33.5
Number of blades	-	4
Main Rotor Revolutions per Minute	rpm	395
Main Rotor Solidity	-	0.07
Tail Rotor Diameter	ft	3.25
Number of blades	-	10
Tail Rotor RPM	RPM	1975
Tail Rotor Solidity	-	0.32
Distance between rotors (estimated)	ft	21.6